Iranian Polymer Journal
20 (5), 2011, 377-387

Available online at: http://journal.ippi.ac.ir

Oxidized Polypropylene Wax in Polypropylene Nanocomposites: A Comparative Study on Clay Intercalation

Ali Salimi[1*], S Mojtaba Mirabedini[1], Mohammad Atai[1], and Mohsen Mohseni[2]

(1) Iran Polymer & Petrochemical Institute, P.O. Box: 14965/115, Tehran-14977/13115, Iran
(2) Department of Polymer Engineering and Color Technology, Amirkabir University of Technology, P.O. Box: 15875/4413, Tehran-15916/34311, Iran

Received 14 March 2010; accepted 19 February 2011

ABSTRACT

Polypropylene-clay nanocomposites were prepared in solution and followed by a melt mixing process. The nanocomposites were prepared for 5% (by weight) organoclay with varying amounts of two oxidized polypropylene waxes (OPPWs) as compatibilizer. The clay dispersion was analyzed by X-ray diffraction (XRD), transmission electron microscopy and melt rheology technique. The extent of intercalation in clay platelets was quantified by XRD analysis based on interactions between OPPW and clay layers. A maximum of ca. 10% increase in clay basal spacing was observed. It was revealed that the degree of clay intercalation in solution technique varies by the polarity of OPPW. In subsequent melt mixing process, the clay dispersion was evaluated by XRD which correlated well with the variations of storage moduli at low frequency region and displayed a pseudo solid-like behaviour. The rheological measurements also showed higher dispersion of clay platelets in PP matrix in the presence of OPPW. The increase in storage moduli especially at low frequency region implied that there were stronger interactions between Cloisite® 15A organoclays and polymer chains when OPPW is present. The TEM images mainly suggested to com-patibilizing effect of OPPW in clay intercalation. In spite of low mechanical properties of OPPW, the DMTA showed the highest modulus of glassy region in nanocomposites with maximum OPPW content. These findings agreed well with each other in co-intercalation effect of OPPW in PP nanocomposites.

Key Words:

polypropylene;
organoclay;
oxidized PP;
polypropylene wax;
intercalation.

INTRODUCTION

In preparation of clay-nanocomposites, a considerable attention has been paid on the intercalation of polymers in layered clay particles. In many areas, complete dispersion of the clay platelets in polymer matrix is an intentional target of the formation process [1-4]. The affinity of polymer segments into the inorganic surface of silicate layer is the key factor in polymer-organoclay interaction. In neat polyolefins such as PP, there is no attraction onto the polar surface of silicate hence resulting in inferior clay dispersion in PP matrix [1,3-5].

In polyolefin based nanocomposites, various approaches including the use of compatibilizers and more polar additives have been introduced. A small amount of polyolefin that has been lightly grafted with maleic anhydride, e.g.,

(*) To whom correspondence to be addressed.
E-mail: a.salimi@ippi.ac.ir

PP-*g*-MA is well documented as an effective compatibilizer for dispersing organoclay in parent polyolefin [1,5-8]. In addition to the polarity, other properties such as molecular weight of the additive play an important role in clay dispersion [1,3,9]. As the polymer-organoclay attraction increases by adding PP-*g*-MA or increasing the content of polar comonomer, the clay stacks become thinner and shorter, hence resulting in higher performance of nanocomposite. In fact, the best dispersion can be attained by optimizing the structure of the additive and processing parameters [10].

There exists extra possibility in clay dispersion by using some specific polar additives combined with PP-*g*-MA. These specific polar additives such as ammonium terminated PP [11], chlorosulphonated PP [12] or hydroxyl functional PP [13] and amide type additive [14] are able to diffuse into clay galleries to promote particle intercalation [15,16]. In recent years, oxidized polyolefins of low molecular weights have been introduced as new types of compatibilizers for preparation of polyolefin-clay nanocomposites by melt processing [17-19]. An oxidized wax in LLDPE/organoclay leads to a noticeable increase in basal spacing. Due to strong interactions between functional groups of the wax chain and organic modifier in clay (Cloisite® 20A), preferable penetration of wax inside the clay layers occurs [17]. The effect of paraffin wax on the dispersion of organically modified montmorillonite (OMMT), was significant for clay concentration higher than 3% (by weight) [20]. The simultaneous increase in stiffness, strength, toughness [20] and also barrier properties [19,21] with the addition of OMMT was recorded in comparison with pristine paraffin wax. In silica nanocomposites, due to stronger interactions between nanosilica and oxidized paraffin wax, maleic anhydride was reported to act more efficiently in clay dispersion. Consequently, higher thermal and mechanical properties of samples can be obtained using oxidized wax and maleic anhydride simultaneously [22]. It was also found that the PE-*g*-MA yielded better clay dispersion compared with oxidized PE [18]. Interestingly, they have reported better oxygen permeability for nanocomposites prepared with oxidized PE than those prepared with PE-*g*-MA with the same sample composition [19].

Much efforts have been devoted to quantifying the dispersion of organoclays in nanocomposites using XRD and TEM techniques [11,23]. However, the combination of these methods together with the results of melt rheology helps to acquire a better understanding of clay dispersion. The effectiveness of rheological properties in the study of nanocomposite morphology has been well documented [4,9,13,14,16,18,19,24-26]. In spite of traditional characterization techniques such as XRD and TEM, melt rheology touches with higher volume of the sample. Unless repetitive, a small area examined by TEM micrograph may not be representative of the overall microstructure [18,23,24]. Besides, the lower cost of rheology offers the possibility in rapid quantifying the extent of clay dispersion in polymer matrix [24,25,27]. The overall pattern of storage and loss modulus in addition to some characteristic parameters such as shear thinning exponent [27] and also crossover frequency offers a valuable method in characterization of the whole exfoliation process [23,25]. It has been shown that an efficient dispersion of OMMT accounts for the emergence of solid-like behaviour and slower relaxation in PP nanocomposites [25,26]. The combination of this technique with the results of XRD and TEM can give reliable information on dispersion state of nanoclays in polymer matrix [25,27].

In this study, the efficiency of OPPW was examined as a new type of compatibilizer for organoclay dispersion in PP matrix. The ability of OPPW in remodification of commercial Cloisite® 15A was studied on OPPW content and the level of polarity. The discussions on clay dispersion were made based on the rheological measurements coupled with common XRD and TEM techniques. The efficiency of rheological measurements as cumulative property was examined in clay dispersion.

EXPERIMENTAL

Materials

Polypropylene (PP) homopolymer was supplied by Navid Zar Chimi (Iran) (MFI 8 g/10 min, at 230°C, 2.16 kg). Two oxidized PP waxes, namely OPPW-1 and OPPW-2, were synthesized from a commercially

available neat PP wax (Coschem Company, Korea) which were reported in details elsewhere [28]. OPPW is a polar low molecular weight polypropylene which contains various oxygen-based functionalities such as carbonyl and hydroxyl groups. The organoclay; Cloisite® 15A (C-15A), treated with a kind of quaternary tallow ammonium salt, was supplied from Southern Clay Products, Inc, USA. Toluene, as solvent for OPPW was used as received from Merck.

Preparation of Polypropylene-clay Nanocomposites

Polypropylene-clay nanocomposites were prepared in two stages. In the first stage, 2 g of OPPW was dissolved in 50 mL toluene and then the organoclay, C-15A (based on 5% by weight of PP) was added while stirring. The mixture was then ultra sonicated for 5 min using probe KE76 in GM 2200 processor. The sonication parameters were 75% power amplitude, a 2-s "pulse on" and 1-s "pulse off". After solvent removal, a master batch of organoclay in OPPW was obtained. In the second stage, different nanocomposites were prepared through the inclusion of master batch into the PP matrix in a 60-mL mixing chamber of Haake SYS 90 (USA). In continuation, the master batches were mechanically broken and mixed well in chamber at 190°C for 10 min at a mixing speed of 80 rpm. Nanocomposite sheets of 2 mm thickness were then prepared using a hydraulic press.

In the first stage, the variables in the formation of master batch were studied using two kinds of OPPW in different wax:clay ratios, i.e., 0.5:1, 1:1, 3:1, 5:1, 7:1 and 10:1 in toluene. It should be noted that the formation of master batches in solution was a time consuming process and care must be paid on environmental considerations.

The physical properties of two kinds of OPPWs are presented in Table 1. As shown in this table,

Table 1. The physical properties of OPPWs utilized in this study [26].

Sample	$\overline{M}_n$ ($g.mol^{-1} \times 10^{-3}$)	Sample (mg KOH/g)
OPPW-1	2.693	8.0
OPPW-2	1.917	13.5

Table 2. Description of the nanocomposite samples.

Sample	PP (% by weight)	OPPW-2 (% by weight)	C-15A (% by weight)
A	95.0	5.0	-
B	95.0	-	5
C	92.5	2.5	5
D	90.0	5.0	5

OPPW-2 denotes oxidized wax with higher acid value hence higher polarity. Despite neat polypropylene, the existing polar groups available on both oxidized waxes facilitate dissolution in toluene at ambient temperature.

In the second stage, the optimum formulation in master batch, based on OPPW-2 and 5% (by weight) of C-15A in PP, was incorporated into the PP matrix. A series of prepared samples are shown in Table 2.

Characterization of Polypropylene-clay Nanocomposites

Wide angle X-ray diffraction (WAXD) was employed to study the microstructure of nanocomposite as well as the extent of clay dispersion using Bragg's law. The technique was performed on a Siemens D5000 diffractometer (Germany) using CuK_α radiation (1.54 Å). Diffraction spectra were obtained at an accelerating voltage of 35 kV and over a 2θ range of 2-10° in steps of 0.01° and counting times of 0.2 s at each angular position. The WAXD spectra were obtained from thin films on lamella and 2 mm thick sheets for master batch and nanocomposites, respectively.

The dispersion and compatibilization of clay particles in PP matrix were also evaluated using TEM employing a Philips EM 208 S (USA) with an acceleration voltage of 120 kV. For TEM sample preparation, injected sheets were microtomed with a glass knife perpendicular to moulding direction.

Viscoelastic behaviour of nanocomposites was analyzed using a MCR 300 dynamic oscillatory rheometer from Anton Paar (Austria). Samples were directly loaded between the parallel plates with a gap distance of 1 mm. The tests were carried out in nitrogen atmosphere and in the temperature range of 180-240°C with 20°C intervals. The strain sweep test

showed a linear viscoelastic region at strain magnitude lower than 0.2%. By applying shear stress (strain magnitude of 0.1%), the storage modulus (G'), loss modulus (G") and dynamic viscosity (η^*) were measured as functions of angular frequency (ω) in the range of 0.01-600 rad/s.

In order to obtain the material response in a broad range of frequency, the principle of time-temperature superposition (TTS) was used. The master curve of sample at specific temperature was generated using the principle of TTS which shifted to reference temperature of 180°C. The reference temperature was chosen at the lowest test temperature to conduct better investigation at low frequency region.

Dynamic mechanical thermal analysis (DMTA) was performed using a Triton (UK) under air atmosphere. The nanocomposites (32×20×2 mm^3) were injected at 210°C using the minimoulder (Dynisco Polymer Test, USA). The DMTA tests were carried out in the temperature range of -100°C to 150°C at a constant rate of 5°C/min and a sinusoidal frequency of 1 Hz.

RESULTS AND DISCUSSION

In order to study the possible effect of toluene on the structure of C-15A, diffraction patterns of pristine organoclay before and after sonication in solvent were examined. The mixture of C-15A organoclay in toluene was sonicated as in a usual process and dried afterwards. XRD Patterns of C-15A prior to and after sonication in the presence of toluene are shown in Figure 1.

As shown in Figure 1, the organoclay C-15A has a major characteristic peak at about $2\theta = 2.6°$ which is indicative of the platelet separation or basal spacing of 31.5 Å. There is also a minor peak at about $2\theta = 7.3°$ corresponding to ordered nanoclay platelets [2,3]. In order to determine the change in maximum basal spacing of pristine C-15A, the d_{001} value of 31.5 Å at about $2\theta = 2.6°$ was compared with the corresponding value of 28 Å at about $2\theta = 3.2°$. In fact, the maximum basal spacing of pristine C-15A decreased to about 3.5 Å after sonication in the presence of toluene. The decrease in basal spacing of C-15A can be attributed to the removal of existing

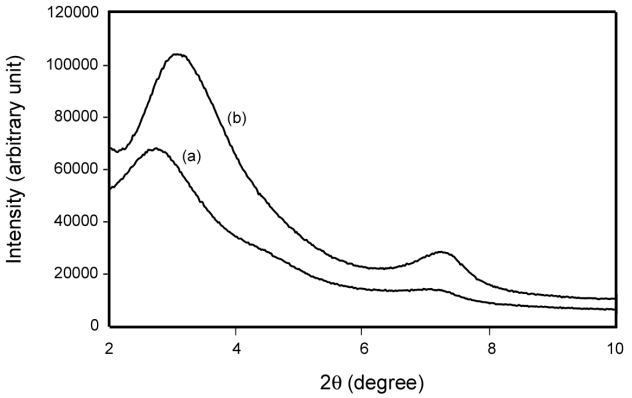

Figure 1. XRD Patterns of pristine C-15A: (a) before and (b) after sonication in toluene.

tallow ammonium salt in clay galleries by toluene. Besides, the change in the colour of the solution after sonication verifies this hypothesis. The solubility parameter (δ) of toluene is 18.2 $(J/m^3)^{0.5}$ and that of tallow ammonium salt is in the range of 18-25 $(J/m^3)^{0.5}$ [29]. It was also reported that toluene may act as extracting solvent in C-15A resulting in platelet spacing of 24.3 Å and more swelling of tallow ammonium salt. This in turn results in more ordered tactoids [29].

According to Figure 1, it seems that the major peak (of maximum basal spacing) of organoclay C-15A after sonication becomes narrower especially in the 2θ range of 4-5.5°. This is in favour of more ordered or stacked tactoids. The lower width in diffraction peak may also be attributed to deviation from mixed-layering in nanoclays [23]. Besides, the intensity of the minor peak at $2\theta = 7.3°$ increases which is an indication of the presence of more ordered tactoids [2,3,29]. In fact, removing more tallow ammonium salt from clay galleries may increase the population of reordered tactoids.

In the next step, the effect of OPPW in toluene was examined on the clay basal spacing. Using the same procedure, two kinds of OPPW with different wax concentrations, i.e., wax:clay ratios, were examined individually. Diffraction patterns of neat OPPW-1 and those of mixtures with different ratios of (OPPW-1:C-15A) are shown in Figure 2.

Due to a low amount of OPPW and hence insufficient wetting of nanoparticles, the wax:clay of 0.5:1 was discarded from further tests. As shown in

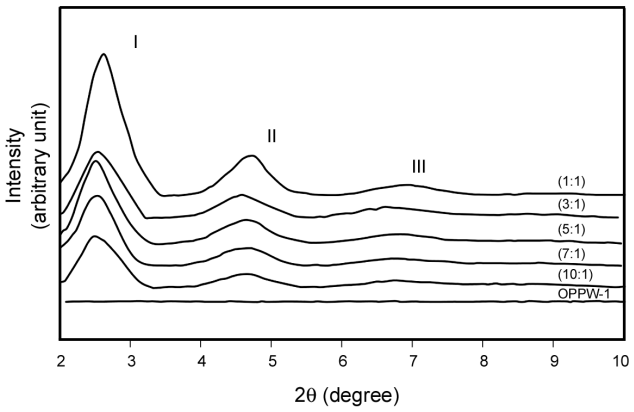

Figure 2. Diffraction patterns of neat OPPW-1 and the mixtures with different ratios of OPPW-1:C-15A.

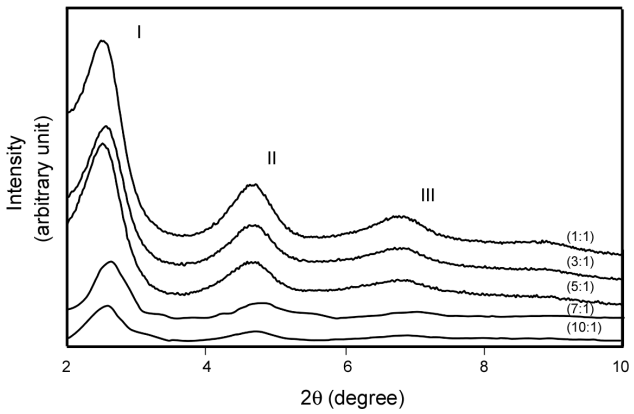

Figure 3. Diffraction patterns of the mixtures with different ratios of OPPW-2:C-15A.

Figure 2, the diffraction pattern of neat OPPW-1 did not diffract throughout the 2θ angles. It can be seen that in all mixtures, the diffraction patterns display three main peaks. The peaks are denoted here as 'peak I' for 2θ = 2.5°, 'peak II' for 2θ = 4.6° and 'peak III' for 2θ = 6.8°. According to Bragg's law, the basal spacings of 34.6 Å, 18.8 Å and 12.9 Å correspond to peak I, peak II and peak III, respectively.

The diffraction patterns of the mixtures with different ratios of OPPW-2:C-15A are shown in Figure 3, which can be seen as the same trend in diffraction patterns of wax:clay as Figure 2. In order to track the changes of diffraction patterns in a quantitative manner, the intensity of each peak was analyzed using the intensity of peak I as a reference. The results of such a comparison are tabulated in Table 3.

As shown in Table 3, in all compositions the maximum basal spacing of organoclay reached about d_{001}= 34.5 Å which suggests for about 10% increase in platelet spacing of pristine C-15A. However, the increase in basal spacing seems to be more for compositions of OPPW-2 compared to those of OPPW-1. In an intercalant such as PP-*g*-MA, the degree of clay exfoliation improves to some extent as the polarity of intercalant increases, which is mainly due to the higher affinity of intercalant to silicate surface [2,3]. The clay basal spacing reached about 40 Å using 6% (by weight) PP-*g*-MA indicating for about 33% increase [15]. The changes in peak ratio for the compositions containing OPPW-1 do not follow a clear trend while for those of OPPW-2 tend to decline. Therefore, it seems that the polarity of OPPW affects clay intercalation.

As shown in Figures 2 and 3, three main peaks appeared in XRD spectra. As stated before, the diffraction pattern of C-15A only showed two main peaks at 2θ angles of 2.6° and 7.3°. In the presence of OPPW, the appearance of one additional peak may be an indication of strong interactions between oxidized

Table 3. The results of diffraction patterns of wax:clay compounds.

Wax:Clay	d_{001} (Å)*		II/I		III/I	
	OPPW-1	OPPW-2	OPPW-1	OPPW-2	OPPW-1	OPPW-2
1:1	33.7	34.5	0.262	0.436	0.074	0.230
3:1	34.5	34.1	0.345	0.417	0.166	0.232
5:1	34.8	34.6	0.285	0.310	0.113	0.165
7:1	33.7	34.5	0.259	0.265	0.105	0.116
10:1	35.0	34.3	0.271	0.270	0.149	0.159

(*) Based on peak I.

wax and clay interlayer surface. Interestingly, no intensive peak was recorded for neat OPPW-1 as shown in Figure 2. In fact, peak II which appears between peak I and peak III gives an indication of partially ordered organoclays. In other words, peak II may be referred to the broadening range of clay basal spacing. The OPPW chains cover a range of molecular weights and as co-intercalant it has higher molecular weight than tallow ammonium salt. The higher molecular weight of intercalant restricts its ability in diffusion into clay galleries causing the characteristic diffraction peak to appear at higher 2θ angles [15]. Therefore, the incorporation of OPPW as co-intercalant of tallow ammonium salt provides wider distribution of molecular weights and appearance of peak II. That is why two close-by diffraction peaks developed for modified clays by using OPPW and tallow ammonium salts at the same time. Even, if one considers the peak II as referred to d_{002}, the position of both d_{001} and d_{002} peaks may be used for degree of clay dispersion [18]. In Figure 2, there is a little shift for peaks I and II to lower angles verifying the positive effect of OPPW in its ability for clay intercalation.

The radius of gyration for OPPW molecules is a required (but not sufficient) condition for diffusing of the wax polymeric chains into clay galleries. Based on the measurements made by Mani et al., the PP molecules having molecular weight lower than 51000 $g.mol^{-1}$ are able to enter into the interlayer spacing of Cloisite® 15A [15]. Assuming the same chain conformation in OPPW as in PP, it is expected that the OPPW molecules could enter the clay galleries of C-15A. As mentioned in Table 1, the molecular weight of OPPW is much below 51000 $g.mol^{-1}$ which favours lower radius of gyration. Therefore, the low radius of gyration of OPPW brings the required condition for entering into interlayer spacing of C-15A. At this stage, the intercalation of OPPW into clay galleries is accomplished by the attraction forces during solvent evaporation.

Briefly, the lower peak ratios together with the increased basal spacing are indications of OPPW ability to intercalation into clay galleries. Although the intercalation of C-15A is not strongly affected by the incorporation of OPPW, the results suggest that the polarity of the wax is a determining factor in the intercalation of the clay platelets.

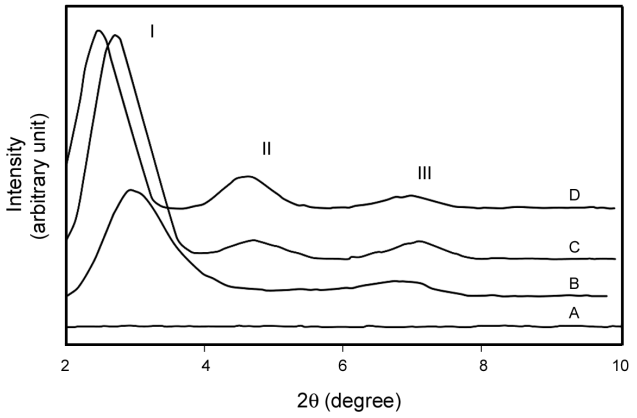

Figure 4. Diffraction patterns of nanocomposites containing OPPW. Sample A (no clay), sample B (no wax), sample C (wax:clay is 0.5:1) and sample D (wax:clay is 1:1).

In preparation of nanocomposites and in the final stage, the master batches were mixed with PP in accordance to Table 1. After melt mixing, the samples were examined for clay intercalation using XRD. The diffraction patterns of samples A, B, C and D are shown in Figure 4.

In XRD patterns of sample A, there is no clay in the matrix and hence no diffraction can be observed in the investigated range (2θ = 2-10°). In sample B, only one main peak corresponding to the basal spacing of about 31 Å can be seen. There was also a minor peak at about 6.8°. In samples C and D an additional peak has appeared at about 4.6° (peak II). As stated before, the appearance of this peak can be attributed to the interactions between organoclay and polymer matrix. In both nanocomposites, containing different levels of OPPWs, the maximum basal spacing increases outmost with the sample D. Sample D shows the greater basal spacing as it contains more oxidized wax. The results of diffraction patterns of samples B, C and D are tabulated in Table 4.

Table 4. The results of diffraction patterns of samples B, C and D.

Sample	d_{001} (Å)	II/I	III/I
B	30.4	-	0.145
C	32.4	0.081	0.085
D	35.1	0.073	0.180

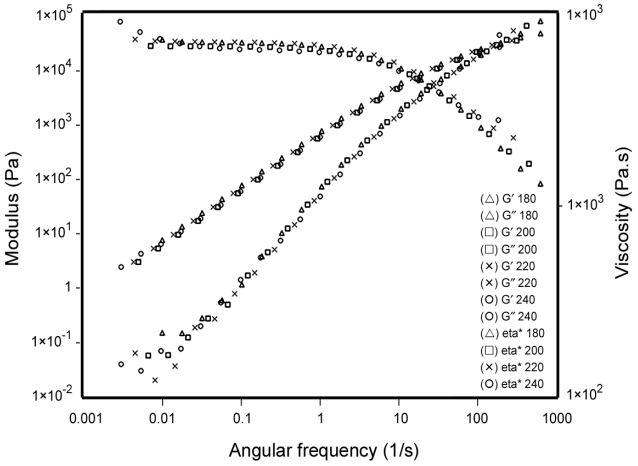

Figure 5. The frequency dependence of storage modulus (G'), loss modulus (G") and complex viscosity (η*) for sample A (no clay).

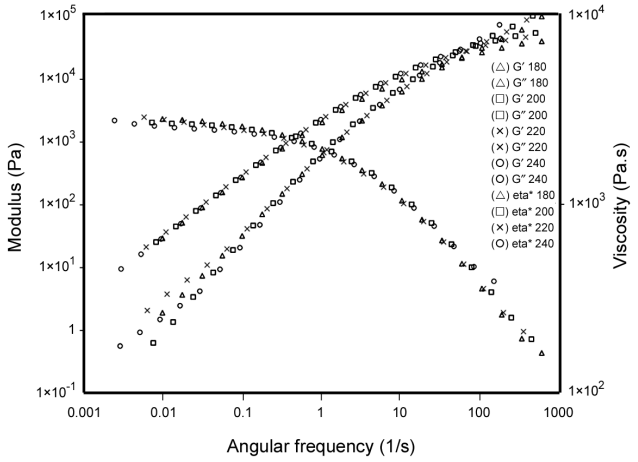

Figure 6. The frequency dependence of storage modulus (G'), loss modulus (G") and complex viscosity (η*) for sample B (no wax).

Referring to Table 4, the basal spacing of sample B is almost the same as pure C-15A. However, in samples C and D, the basal spacing increases. In sample D, the basal spacing reaches its maximum value. The peak ratios decreased a little due to small alteration of organoclays. The results are in favour with the positive effect of OPPW in clay intercalation.

In the next step, the clay dispersions were studied using oscillatory shear rheology. At first, the dynamic strain sweep test was applied to samples to determine linear viscoelastic region. A strain of 1% amplitude was then set for all tests. The rheological measurements of samples A, B, C and D are shown in Figures 5 to 8, respectively.

The overall patterns of G', G" and intrinsic viscosity can be seen in all dynamic mechanical spectra. In the study of nanocomposite structure, the storage modulus (G') has been reported to be more sensitive than the loss modulus (G") [18].

In the spectra of all samples, only one crossover point was associated at frequencies of about 100 Hz showing for two distinct regions. The terminal modulus of G' of sample A was higher than that of sample B. It is shown that the incorporation of organoclays eagerly increases the terminal modulus of G' from 0.04 Pa for sample A to 0.55 Pa for sample B (at the frequency of 0.003 Hz). The increase in G' is more significant in the samples C and D and reaches about 3.1 Pa for sample D (at the frequency of 0.003 Hz). The comparison of the results of G' for the samples C and D with those of sample B shows that organoclay has a more pronounced filler effect using OPPW in spite of its low molecular weight and hence low melt viscosity. It seems that the incorporation of more OPPW into polymer would result in greater change in the spectrum of terminal relaxation region. The G' approaches a slope of unity in low frequency region (assigned by dash line in sample D) indicating a pseudo solid-like behaviour. The

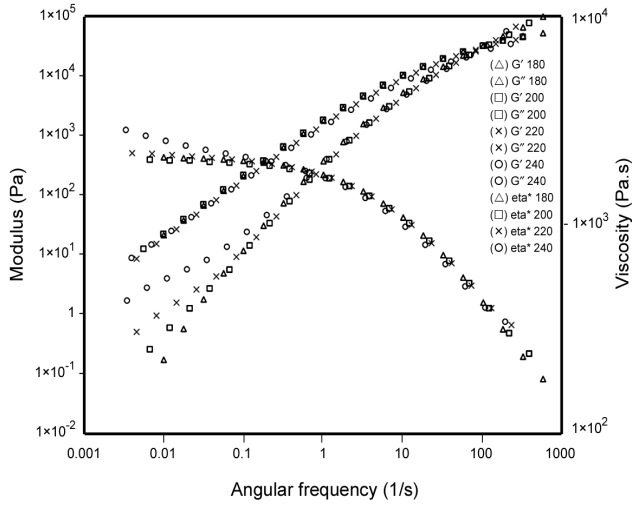

Figure 7. The frequency dependence of storage modulus (G'), loss modulus (G") and complex viscosity (η*) for sample C (wax:clay is 0.5:1).

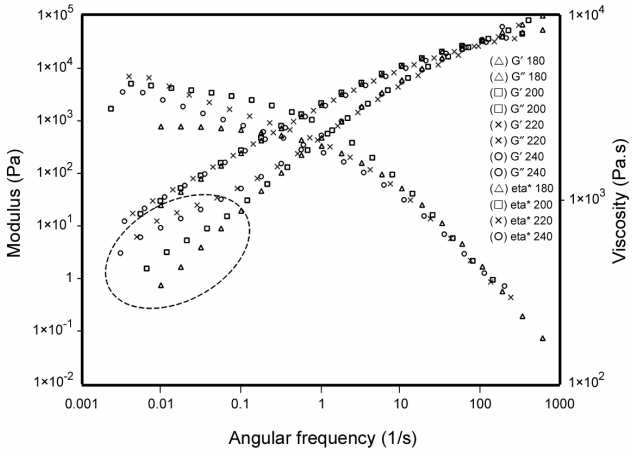

Figure 8. The frequency dependence of storage modulus (G'), loss modulus (G") and complex viscosity (η*) for sample D (wax:clay is 1:1).

improvement of G' at low frequency region can be attributed to delay in complete polymer relaxation [16,24]. The high population of slow relaxing chains is responsible for the low frequency solid-like behaviour of composites. This behaviour and magnitude of G' enhancement at low frequency region may be due to higher interaction of organoclay and polymer chains because of more efficient clay dispersion. In fact, the population of clay particles is the determining factor for this characteristic response of nanocomposites. Briefly, the rheological responses imply that there is a stronger interaction between C-15A and polymer chains using OPPW.

The shear thinning exponents were measured using the logarithmic plot for power law expression. The results were not meaningful for providing a credible characterization of overall clay exfoliation. The data are not shown here for the sake of brevity.

Another direct method involved was TEM for visual observation of nanocomposite morphology. Different images at different points were taken to represent a good evaluation of clay dispersion. In all samples there were different degrees of clay intercalation ranging from clay agglomeration to fully exfoliation. However, the mechanism of clay intercalation can be regarded as a valuable feature in TEM images. Therefore, the microimages of TEM were employed for the investigation of the mechanism of clay intercalation. The TEM images of samples B, C and D are shown in Figure 9.

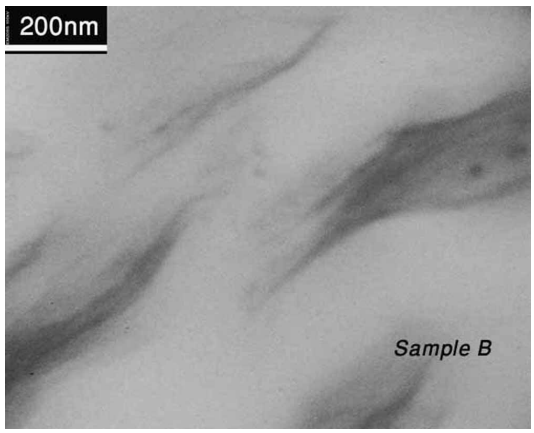

(a)

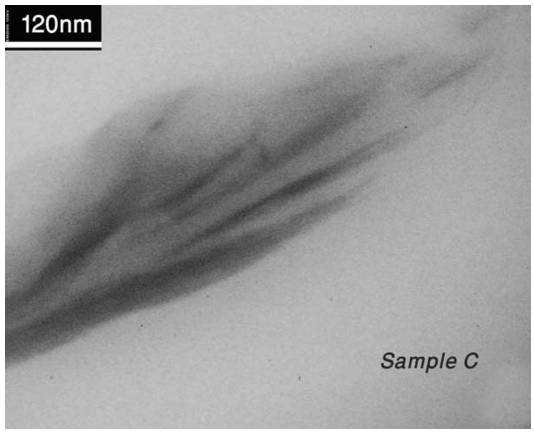

(b)

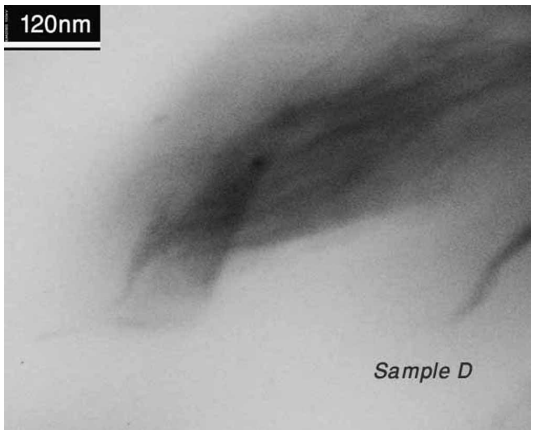

(c)

Figure 9. TEM Micrographs of samples: (a) B (no wax), (b) C (wax:clay 0.5:1) and (c) D (wax:clay 1:1).

As shown in Figure 9, the intercalation into a single clay stack can be observed in all samples. Based on the intercalation mechanism proposed by Pavildoua et al., the clay intercalation is a function of chemical compatibility between clays and matrix and also of processing conditions [3]. Due to similar melt

mixing procedure for all samples, the chemical nature of the matrix plays a key role in clay intercalation. In the presence of high intensive shear forces, the clay platelets may slide apart from each other, i.e., they shear apart. Accordingly, the stacks are decreased in height. In the case of more compatibility between species, the polymer chains enter into clay galleries at the ends of platelets stacks pushing them apart, i.e., they peel apart each other. This pathway does not need high shear intensity but involves diffusion of polymer into clay galleries [3].

In this study, it is proposed that the diffusion into the clay galleries is mainly driven by the physical and chemical attraction of OPPW for organoclay surface. As shown in Figure 9a, the clay stacks mainly shear apart and become narrower in sample B. In this case, the clay intercalation is attained mainly by shear forces present in process. In system with lower chemical compatibility, the processing condition has the major effect on intercalation of clays. In the samples such as C and D which contain OPPW, the clay stacks mostly peel apart from each other. The clay intercalation is mainly due to increased compatibility of the system in these samples. The mechanism is a time consuming process and depends on the amount of OPPW present. Briefly, the behaviour of peel apart indicates compatibilizing effect of OPPW in samples C and D.

Mechanical response of nanocomposites over a range of temperatures was characterized by DMTA. The technique may be used for rich explanation of clay dispersion. The resulting curves for samples A, B, C and D are shown in Figure 10.

In general, all samples showed a similar trend. They have only one peak as clearly reflected in loss factor curves. The single peak in loss factor curves can be an indication of single phase blend. The maxima in peak slightly differs with the least amount for sample D. Hence, the lowest glass transition temperature of 21°C is attributed to sample D. The damping peak also broadens to some extent for sample C, which might be due to the plasticizing effect of wax [22,28]. However, the storage moduli at glassy region were higher for samples B, C and D compared to sample A. This may be due to filler effect of organoclays and subsequent interactions with polymer chains in these samples. An interesting

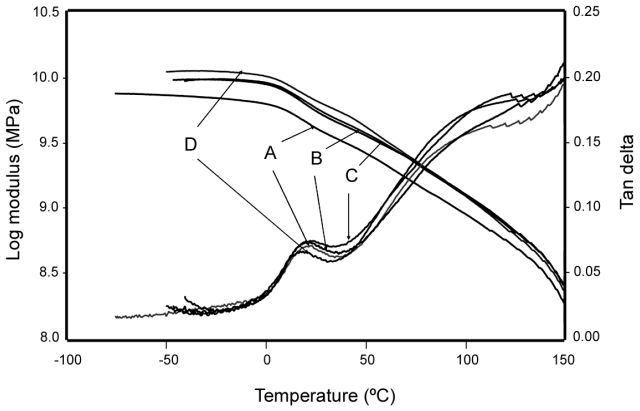

Figure 10. The moduli and loss factor curves for samples: A (no clay), B (no wax), C (wax:clay 0.5:1) and D (wax:clay 1:1).

finding is that the maximum modulus corresponds to sample D among the others in which it has the highest wax content (at the same level of organoclay, i.e., 5% by weight). As the temperature approaches the glassy region, the storage modulus of sample D experiences extra change. In fact, the higher modulus in sample D may be attributed to better dispersion of organoclay in polymer matrix. The result of DMTA is in agreement with the results of XRD and rheology measurements which are capable to predict the efficiency of OPPW in dispersion of clay platelets in PP matrix.

CONCLUSION

The formation of nanoclay master batches in solution state and subsequent melt mixing in polymer is an applicable procedure in preparation of polypropylene-clay nanocomposites. A study on XRD spectra of pristine C-15A showed that the quaternary ammonium ion salt used in C-15A is soluble in toluene. It may lead to an obvious reduction in maximum basal spacing after sonication. The approach in XRD method was to compare the quantifiable features in XRD analysis, i.e., *d*-spacing and peak intensity. These parameters were used efficiently as an indicator for OPPW co-intercalation effect. The ability of OPPW in remodification of commercial Cloisite® 15A nanoclays was found to be dependent on OPPW content and the level of

polarity. In mixtures prepared through solution procedure, the *d*-spacing of the largest basal reflection showed almost the same improvement for different wax:clay ratios. A maximum of about 10% increase in *d*-spacing was recorded which indicated to lower efficiency of OPPW comparing to PP-*g*-MA counterpart [15]. In melt intercalation method, the material with higher OPPW content appeared to have higher *d*-spacing. In comparison with the neat PP-organoclay compound, the storage modulus at low frequency region was higher in all OPPW containing nanocomposites. The population of organoclay particles dominates the rheological response of nanocomposites. The TEM images confirmed the compatibility effect of OPPW in clay intercalation. The discussions on clay dispersion based on common XRD and TEM techniques were strengthened by the rheological measurements. The DMTA results also showed a good description of OPPW influence on the storage modulus of nanocomposite in glassy region. Incorporation of more OPPW into polymer would result in higher storage modulus in the glassy region due to more efficient dispersion of organoclay particles.

REFERENCES

1. Paul DR, Robeson LM, Polymer nanotechnology: nanocomposites, *Polymer*, **49**, 3187-3204, 2008.
2. De Pavia LB, Morales AR, Valenzuela Diaz FR, Organoclays: properties, preparation and applications, *Appl Clay Sci*, **42**, 8-24, 2008.
3. Pavlidoua S, Papaspyrides CD, A review on polymer-layered silicate nanocomposite, *Prog Polym Sci*, **33**, 1119-1198, 2008.
4. Rohlmann CO, Horst MF, Quinzani LM, Failla MD, Comparative analysis of nanocomposites based on polypropylene and different montmorillonites, *Eur Polym J*, **44**, 2749-2760, 2008.
5. Chiu F-C, Yen H-Z, Lee C-E, Characterization of PP/HDPE blend-based nanocomposites using different maleated polyolefins as compatibilizers, *Polym Test*, **29**, 397-406, 2010.
6. Yuan M, Guo M, Miao Z, Liu Y, Influence of maleic anhydride grafted polypropylene on the dispersion of clay in polypropylene/clay nanocomposites, *Polym J*, **42**, 745-751, 2010.
7. Varela C, Rosales C, Perera R, Matos M, Poirier T, Blunda J, Rojas H, Functionalized polypropylene in the compatibilization and dispersion of clay nanocomposites, *Polym Compos*, **27**, 451-460, 2006.
8. Mehrabzadeh M, Kamal MR, Quintanar G, Maleic anhydride grafting onto HDPE by in situ reactive extrusion and its effect on intercalation and mechanical properties of HDPE/clay nanocomposites, *Iran Polym J*, **18**, 833-842, 2009.
9. Wang Y, Chen FB, Wu KC, Wang JC, Shear rheology and melt compounding of compatibilized- polypropylene nanocomposites: effect of compatibilizer molecular weight, *Polym Eng Sci*, **46**, 289-302, 2006.
10. Li P, Song G, Yin L, Sun C, Wang L, Study on structure-property relationships of polypropylene/OMMT nanocomposites with different morphologies, *Iran Polym J*, **16**, 775-785, 2007.
11. Wang ZM, Nakajima H, Manias E, Chung TC, Exfoliated PP/clay nanocomposites using ammonium terminated PP as the organic modification for montmorillonite, *Macromolecules*, **36**, 8919-8922, 2003.
12. Kotek J, Kelnar I, Studenovsky´ M, Baldrian J, Chlorosulfonated polypropylene: preparation and its application as a coupling agent in polypropylene-clay nanocomposites, *Polymer*, **46**, 4876-4881, 2005.
13. Ristolainen N, Vainio U, Paavola S, Torkkeli M, Serimaa R, Seppala J, Polypropylene/organoclay nanocomposites compatibilized with hydroxyl-functional polypropylene, *J Polym Sci Part B: Polym Phys*, **43**, 1892-1903, 2005.
14. Haworth B, Ratnayake U N, Co-intercalation in PP clay nanocomposites: effect of short chain additives on rheological properties, *Int Polym Process*, **01**, 91-99, 2011.
15. Mani G, Fan Q, Ugbolue SC, Yang Y, Morphological studies of polypropylene-nanoclay composites, *J Appl Polym Sci*, **97**, 218-226, 2005.
16. Dal Castel C, Bianchi O, Oviedo MAS, Liberman SA, Mauler RS, Oliveira RVB, The influence of interfacial agents on the morphology and viscoelasticity of PP/MMT nanocomposites, *Mater Sci Eng C*, **29**, 602-606, 2009.

17. Luyt AS, Geethamma VG, Effect of oxidized paraffin wax on the thermal and mechanical properties of linear low-density polyethylene-layered silicate nanocomposites, *Polym Test*, **26**, 461-470, 2007.
18. Durmus A, Kasgoz A, Macosko CW, Linear low density polyethylene (LLDPE)/clay nanocomposites. Part I: Structural characterization and quantifying clay dispersion by melt rheology, *Polymer*, **48**, 4492-4502, 2007.
19. Durmus A, Woo M, Kasgoz A, Macosko CW, Tsapatsis M, Intercalated linear low density polyethylene (LLDPE)/clay nanocomposites prepared with oxidized polyethylene as a new type compatibilizer: structural, mechanical and barrier properties, *Eur Polym J*, **43**, 3737-3749, 2007.
20. Wang J, Severtson SJ, Stein A, Significant and concurrent enhancement of stiffness, strength and toughness for paraffin wax through organoclay addition, *Adv Mater*, **18**, 1585-1588, 2006.
21. Chiko DJ, Leyva AA, Thermal transitions and barrier properties of olefinic nanocomposites, *Chem Mater*, **17**, 13-19, 2005.
22. Motaung TE, Luyt AS, Effect of maleic anhydride grafting and the presence of oxidized wax on the thermal and mechanical behavior of LDPE/silica nanocomposites, *Mater Sci Eng A*, **527**, 761-768, 2010.
23. Eckel DF, Balogh MP, Fasulo PD, Rodgers WR, Assessing organo-clay dispersion in polymer nanocomposites, *J Appl Polym Sci*, **93**, 1110-1117, 2004.
24. Zhao J, Morgan AB, Harris JD, Rheological characterization of polystyrene-clay nanocomposites to compare the degree of exfoliation and dispersion, *Polymer*, **46**, 8641-8649, 2005.
25. Krishnamoorti R, Yurekli K, Rheology of polymer layered silicate nanocomposites, *Current Opinion in Coll Int Sci*, **6**, 464-470, 2001.
26. Banerjee S, Joshi M, Ghosh AK, Spectroscopic approach for structural characterization of polypropylene/clay nanocomposite, *Polym Compos*, **31**, 2007-2016, 2010.
27. Wagener R, Reisinger TJG, A rheological method to compare the degree of exfoliation of nanocomposites, *Polymer*, **44**, 7513-7519, 2003.
28. Salimi A, Mirabedini M, Atai M, Mohseni M, Studies on the mechanical properties and practical coating adhesion on PP modified by oxidized wax, *J Adhes Sci Technol*, **24**, 1113-1129, 2010.
29. Ho DL, Briber RM, Glinka CJ, Studies of organically modified clays by scattering techniques, In: *Polymer Nanocomposites Synthesis, Characterization, and Modeling*, Krishnamoorti R, Vaia RA (Eds), ACS Symp Ser, **804**, 127-140, Houston, 2002.